

## Modeling Minimum-Time Maneuvering with Global Optimization of Local Receding Horizon Control

Jeffery Ryan Anderson<sup>a\*</sup> and Beshah Ayalew<sup>a</sup>

<sup>a</sup>*Department of Automotive Engineering, Clemson University, Greenville, SC, USA*

In this paper, we explore the notion that a human driver uses a receding horizon model predictive control (MPC) scheme for minimum-time maneuvering. However, MPC is an inherently sub-optimal control scheme because not all future information is incorporated into its finite preview horizon. In many practical applications, this sub-optimality is tolerated as the solution is sufficiently close to optimal. However, it is known that professional drivers have the ability to learn driving circuits and exploit its features to minimize their global maneuvering time. In this paper, we will model their process with a cascaded optimization structure. Therein, the inner-loop features a local MPC scheme tasked with finding the control inputs that achieve a blended objective of minimizing time and maximizing velocity in each preview horizon/distance. The outer-loop of this cascaded structure computes the best set of weights for the two components of the local objectives in order to minimize the global maneuvering time. The proposed cascaded optimization and control approach is compared against a straight-forward fixed-cost time optimal MPC applied to minimum-time maneuvering over two well-known race courses. The paper also includes an extended literature review and details of the computational formulation of the model approach.

**Keywords:** Model predictive control; driver modeling; vehicle dynamics; minimum-time maneuvering; professional drivers

### 1. Introduction

Minimum-time vehicle maneuvering is an important sub-set of studies in vehicle dynamics and has a very direct influence on the motorsports industry [1]. It also influences other aspects of the automotive sector especially for modern high performance automobiles. Moreover, knowledge gained here indirectly affects a much larger aspect of vehicle design such as safety and driver assistance systems. The modeling and understanding of how high-performance human drivers manage to operate efficiently despite the very nonlinear dynamics involved in minimum-time maneuvers can provide useful insights for future implementations of autonomous vehicle controllers as well.

This paper presents a cascaded optimization structure which is intended to model a professional driver learning a new driving circuit to minimize maneuvering time. The inner loop of this structure features a blended cost receding horizon model predictive control (MPC) that is capable of weighting different objectives in each horizon. MPC is chosen as the control strategy for the inner loop based on the some recent justifications for how it closely represents human-driver actions. Casanova [2] makes the case that a human driver behaves more like a MPC (in a moving horizon manner) than an optimal

---

\*Corresponding author. Email: jra3@clemson.edu

controller acting on the full maneuver. He states, if a driver were indeed a true optimal controller acting over the entire circuit then, he or she will choose his initial control inputs on the start line based on how he or she intends on crossing the finish line. Since a driver is clearly not using the full racing circuit to that extent in order to make control decisions, a different mechanism must be in place. Moreover, it was stated in [3], ‘there comes a point where the track ahead has diminishing importance for control decisions affecting the present time.’ In other words, a human is not considering the full circuit when making local control decisions but rather utilizing a preview horizon. While we conjecture that a human driver behaves more like MPC than optimal control, we also know that a human can learn new race tracks to best exploit its features and minimize the global maneuvering time. In order to accomplish modeling of this learning, we expand the local MPC cost function to have two objectives: minimizing time and maximizing velocity at the end of the horizon. These two objectives were motivated by literature where [4] states, it can be advantageous in a short segment to drive with one or the other objective (minimizing time or maximizing velocity) depending on the future track configuration. For example, on a track with a curve followed by a long straight section, it can sometime be advantageous to the global maneuvering time to take more time in the current curve and maximize velocity of corner exit to achieve more speed through the following straight section. The outer loop in our algorithm does just that. It acts on the full track to find the best set of weights that trade-off the two objectives on each MPC horizon for minimal global time. In this direction, our previous work [5] has shown advantages for a hybrid (switching) cost function using a very simple vehicle model and a short section of track. However, the discontinuous switching may be unrealistic. The present work incorporates the ability to more naturally and smoothly blend two local objectives, a more detailed vehicle dynamics model, and much longer driving circuits.

In addition to more closely representing a human driver, MPC has another key computational benefit: the initial guess. Nonlinear optimization in general relies on an initial guess as a starting point to begin searching. The initial guess of the solution is paramount to performance of the computational framework. If this initial guess is too far from the actual solution, the optimization could become computationally very expensive, or worse, fail to converge. With MPC, the only initial guess required is that of the first preview horizon and not the full maneuver as each subsequent horizon can be seeded with the initial guess of the solution to the previous. Therefore, if the first segment is in a location where we know what the driver is doing, for instance, a long straightway where full throttle is applied, then the initial guess should be sufficiently close to the solution in that horizon. This is much easier than guessing a good solution around a full track. The work in [6] originally used this feature of MPC to extend solutions over a short segment to an arbitrarily long track.

In summary, in this paper, we formulate and detail a cascaded optimization scheme of local MPC costs to represent a human learning how to drive a new driving circuit to globally minimize maneuvering time. We will discuss how this cascaded control structure compares with the traditional fixed-cost time-optimal MPC applied around the track. The rest of the paper is organized as follows. Section 2 presents a literature review of relevant work on minimum-time maneuvering. Section 3 details the vehicle model used and cascaded optimization framework. Section 4 presents results on a full race track while section 5 offers conclusions and an outlook on our future work.

## 2. Literature Review

Mercedes Benz is credited with the first engineering formulations for solving lap time simulations [7] dating back to the 1930s. The solution methods that have since been proposed for solving minimum-time maneuvering problems can be classified into three distinct categories. First, the performance envelope method which relies on a steady state assumption of the vehicle performance envelope and neglects the influence of the driver altogether. In order to incorporate the driver effect, the next category, the two-stage path planning/path following methods, were proposed. These methods provide an efficient solution to this problem; however, they rely on the assumption of a fixed racing line. The final category, the one-stage trajectory optimization approach, utilizes optimal control theory to find the optimal control inputs to negotiate a path in minimum time. In this method, the racing line is an output of the optimization. In the subsequent subsections, the three major categories of solution methods will be discussed in detail. This will be followed by motivations for the approach we propose in this paper.

### 2.1. *Performance Envelope Methods*

The steady state performance envelope of a vehicle can be used to generate an optimal velocity profile around a racing track and provide a measure of lap time. This solution technique neglects the driver's behavior and inherently the vehicle transient effects. In its simplest form, a racing circuit could be broken down into a series of straight segments and constant radius turns. Knowing the peak lateral acceleration of the vehicle and a corner radius, a maximum speed could be calculated for each turn. Since the cornering speed in each turn is known, the remainder of the problem is to find the optimal longitudinal speed profile which connects these turns. This is typically done by finding the switching point between full throttle and full brake on these straights. In the early days of racing, the performance envelop of the vehicle was considered relatively independent of speed making a non-iterative solution possible. This was discussed in literature as early as the 1950s [8]. Once the the full velocity profile around the track is known it can be integrated to provide the measure of lap time. As time progressed, these solutions were extended in order to capture higher-order vehicle dynamic effects and more accurate transitions between the cornering and straight segments. Examples of these quasi-steady state (QSS) simulations are abundant in literature and a few key examples are given in: [9–13].

### 2.2. *Two Stage Path Planning/Path Following*

In the general automotive space, driver modeling took quite a different approach than lap simulation. The origins are rooted in the mathematics of modeling aircraft pilots. One of the first driver models of note is the crossover model [14] which utilizes a simple experimentally derived transfer function to model a driver's control actions during regulation tasks such as negotiating a straight section of highway. While this type of driver model is inadequate for the needs of modeling ultra-high performance maneuvers, it is noteworthy because even more modern optimal preview control techniques reduce to the crossover model for regulation tasks [15, 16]. In the context of minimum-time vehicle maneuvering, the optimal preview control formulation proposed in [17] is of significant historical value; this approach can still be found in commercially available software today such as CarSim [18]. Driver modeling itself is a very general field and has several superb review articles that the reader is referred to [19–21] for more detail.

In order to incorporate the driver modeling into minimum-time maneuvering simulations, a two-stage approach can be employed which consists of separate path planning and path following phases. In this approach, the path planning is typically conducted a priori via optimization techniques or even with the use of actual driving telemetry. A common path planning technique is to apply the previously mentioned quasi steady-state lap simulations to adjust the racing line within the track bounds to find the path that yields the best time. In this approach, the driving circuit is divided into waylines and a basis function such as splines can be manipulated at control points along these waylines until an optimal line is found. Examples of this approach can be found in [22]. Other optimization methods neglect all vehicle information and rely solely on path geometry. After all, minimum-time maneuvering is about traveling the shortest distance while achieving the highest speed possible. The work presented in [23–26] provides good examples of choosing a racing line purely on geometric optimization.

Once the racing line is known, the path following stage is employed. Typically optimal preview control techniques rooted in McAdam's optimal preview control [17] are utilized to follow a given path. A good example of this approach can be found in [16]. In [27, 28], a formal mathematical solution was given to this problem. More recently, in [29] it is shown that for a fixed path, the time-optimal velocity profile could be posed and solved as a convex optimization problem. This is a key problem found in robotics [30] and [29] extended this technique for simulation of vehicles.

### **2.3. Trajectory Optimization**

The final category of methods is the one-stage trajectory optimization where the driver is modeled as a pure time-optimal controller. The methods attempt to find the optimum control inputs (i.e., steering, throttle, braking, etc.) to minimize maneuvering time subject to the prevailing vehicle dynamics and road constraints. This line of work began in the early 1990s [31] and [32] may be considered the first significant formulations of these problems. At the same time as Hendrix et al., Da Lio published a very similar work for motorcycles [33]. The work in [3] provides an excellent background into on this topic. Once the optimal control problem is posed, one of two classes of solution methods are employed, which are reviewed in detail in [34]. We briefly touch on this as it relates to our own approach.

The first of these solution methods are indirect methods which aim at finding a solution to the first-order necessary conditions of optimality via application of Pontryagin's Minimum Principle. The problem resulting from these indirect methods is a Hamiltonian boundary value problem which in general is quite arduous to solve. Still, there are many works offering examples of using the indirect methods [32, 33, 35], extensive study of differentials [36], gear ratios [37, 38], racing karts [39], varying model fidelity [40] and vehicle layouts [41].

The second class of solution methods are direct methods which aim at solving the actual optimal control problem instead of deriving the necessary conditions. This is generally done by transforming the optimal control problem into one of a Nonlinear Programming Problem (NLP) via discretization and numerical simulation of the constraints [42, 43]. This method has been used since the late 1990s to solve minimum-time vehicle maneuvering problems [44] and much of the modern work is rooted in [45]. Direct methods have been utilized to research many problems in minimum time vehicle maneuvering. Sensitivity studies were examined in [46] and showed good correlation between practical observations to simulation. Vehicle setup parameter optimizations were performed in [47, 48].

There is discussion on which method is more suited to this problem [3]; however, both methods have yielded excellent results. Moreover, the work in [49], shows that the Lagrange multipliers used in direct methods are discrete approximations of the co-state variables found in the indirect methods and with either method, numerical methods are required (for all but very simple systems) to solve the problem.

In addition to the previously mentioned examples, trajectory optimization has been utilized to analyze many specific vehicle dynamics issues. These include evaluation of different vehicle and tire models and their affect on performance [50–52], motorcycle dynamics in [53, 54], a thermally-dependent tire model [55, 56], kinetic energy recovery systems [34, 57] and torque allocation for the case of individual wheel motors in [58]. Optimization of vehicle parameters along with trajectory planning was studied [59]. Modeling a race circuit in three dimensions was studied in [60] and real-time control has been studied in [61–64].

The main difficulty that comes from using the trajectory optimization methods is that posing an optimal control problem over an entire race circuit or full track is quite a complex problem; however, using state of the art solvers and a good initial guess, a solution can be accomplished [59]. To make the problem tractable, the full track is typically broken down into short segments, which are then concatenated via different methods including multiple shooting [2] or MPC [6].

#### **2.4. Modeling the Human Aspect of Driving**

Modeling the human aspect of driving is not a new topic of study. In fact, several works have presented methods that aim at reproducing the human element of driving. First, the work by Prokop [65] showed how different driving styles can be modeled via different cost functions in a MPC framework. Although his work aimed at a much larger set of driving (not just minimum-time), he was able to model different driving styles from energy saving, to comfort-oriented, and even time-optimal driving. Kelly [66] showed how control discretization is analogous to human control bandwidth and studied the performance tradeoff between control bandwidth and maneuvering time. Robust, tube-based MPC was used to model drivers in [67] in the presence of disturbances. This work also further explores the tradeoff between lap time performance versus driver workload. In [68, 69], the authors demonstrate novel means to pose boundary conditions or change of the performance index in order to model a particular driving style: the trail-braking maneuver. This maneuver is common in rally racing to negotiate sharp turns in blind conditions where a driver will brake while steering and negotiate the corner at a high side slip angle to minimize the heading error at the corner exit and maintain good visibility.

The above reviewed literature supports the utility of MPC for modeling the human-driver not just as a time-optimal controller. More likely, the driver is considering multiple objectives and blending them appropriately in key locations around the race track. Thus, in this work, we use blended objectives that can vary over the race track and pose a global optimization of these objectives to achieve minimal maneuvering time.

### **3. Mathematical Framework**

This section will detail both the vehicle model used for this work and the cascaded optimization structure. The vehicle model consists of a four wheel vehicle model including effects of load transfer, nonlinear tires, aerodynamics, and a differential. The vehicle model will be presented in section 3.1. The cascaded optimization structure consists of

an inner loop MPC controller which drives the vehicle around the track while minimizing its local cost function while the outer loop finds the best cost function for each horizon. This will be further detailed in section 3.2. Finally, we briefly describe a time-optimal MPC controller in section 3.3 to compare the cascaded optimization to.

### 3.1. Vehicle Model

This work utilizes a four wheel vehicle model. The sprung mass has three degrees of freedom: longitudinal velocity ( $v_x$ ), lateral velocity ( $v_y$ ), and rotation about the yaw axis ( $\psi$ ). The wheel dynamics are modeled with four individual differential equations. The following subscripts are used to denote wheel position:  $(\cdot)_p$  where  $p \in \{fl, fr, rl, rr\}$  denotes front left, front right, rear left, rear right wheel position respectively. Much of the vehicle modeling is similar to those used in previous works [36, 59, 66]:

$$\dot{v}_x = v_y \dot{\psi} + \frac{F_x}{m} \quad (1)$$

$$\dot{v}_y = -v_x \dot{\psi} + \frac{F_y}{m} \quad (2)$$

$$\begin{aligned} I_{zz} \ddot{\psi} = & a(\cos(\delta)(F_{y_{fr}} + F_{y_{fl}}) + \sin(\delta)(F_{x_{fr}} + F_{x_{fl}})) + \\ & w_f(F_{y_{fr}} \sin(\delta) - F_{x_{fr}} \cos(\delta)) + \\ & w_f(F_{x_{fl}} \cos(\delta) - F_{y_{fl}} \sin(\delta)) + \\ & w_r F_{x_{rl}} - b(F_{y_{rr}} + F_{y_{rl}}) - w_r F_{x_{rr}} \end{aligned} \quad (3)$$

where  $F_x$  and  $F_y$  denote the total lateral and longitudinal forces acting at the Center of Gravity (Cg):

$$\begin{aligned} F_x = & \cos(\delta)(F_{x_{fl}} + F_{x_{fr}}) - \sin(\delta)(F_{y_{fl}} + F_{y_{fr}}) \\ & + F_{x_{rl}} + F_{x_{rr}} + F_{ax} \\ F_y = & \cos(\delta)(F_{y_{fl}} + F_{y_{fr}}) + \sin(\delta)(F_{x_{fl}} + F_{x_{fr}}) \\ & + F_{y_{rl}} + F_{y_{rr}} \end{aligned} \quad (4)$$

and the individual tire lateral and longitudinal forces are denoted by  $F_{x_p}$  and  $F_{y_p}$ . The distance from the Cg to front and rear axle are  $a$  and  $b$  respectively, half the front and rear track width are  $w_f$  and  $w_r$ , and the front steering angle is  $\delta$  as seen in Figure 1. Aerodynamic drag is  $F_{ax}$  and discussed below.

The remaining four degrees of freedom are comprised of the individual wheel dynamics.

$$\dot{\omega}_{fl} = \frac{(-T_{fl} + R_f F_{xfl})}{Jr_f} \quad (5)$$

$$\dot{\omega}_{fr} = \frac{(-T_{fr} + R_f F_{xfr})}{Jr_f} \quad (6)$$

$$\dot{\omega}_{rl} = \frac{(-T_{rl} + R_r F_{xrl})}{Jr_r} \quad (7)$$

$$\dot{\omega}_{rr} = \frac{(-T_{rr} + R_r F_{xrr})}{Jr_r} \quad (8)$$

### 3.1.1. Vehicle Controls

The lateral and longitudinal dynamics are controlled through inputs:  $u_1$ ,  $u_2$  which is the steering rate and torque demand rate on the chassis. This allows for a convenient mechanism of placing state constraints representing the human bandwidth of control and vehicle limitations. The steering angle and torque demand quantities satisfy:

$$\dot{\delta} = u_1 \quad (9)$$

$$\dot{T} = u_2 \quad (10)$$

The vehicle is assumed to have only front wheel steering. In other words,  $\delta_{fl} = \delta_{fr} = \delta$  and  $\delta_{rl} = \delta_{rr} = 0$ . The torque allocation between the four wheels is modeled based on the work in [70] and depends on whether or not the vehicle is braking or accelerating. While driving, this vehicle is rear-wheel drive only; however, under braking, the brake forces are distributed among all four wheels. Because of this, the torque allocation ( $T$ ) is separated into positive components:  $T^+$ ,  $T^-$ . For our purposes, the following separation method was used.

$$T^+ = \frac{1}{2} + \frac{1}{2} \sin(\arctan(100 \cdot T)) \quad (11)$$

$$T^- = \frac{1}{2} - \frac{1}{2} \sin(\arctan(100 \cdot T)) \quad (12)$$

When it is known whether the vehicle is braking or driving, the torque distribution ( $k_t$ ) can be determined via:

$$k_t = T^+ kt_{driving} + T^- kt_{braking} \quad (13)$$

where the parameters  $kt_{driving}, kt_{braking}$  are fixed vehicle parameters. Finally, the wheel

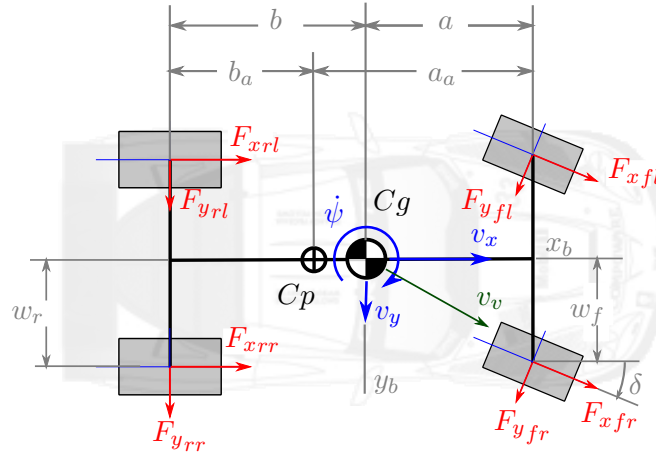


Figure 1. Vehicle top view. Note: body-fixed coordinates  $x_b$  and  $y_b$  are located vertically at the ground plane.

torques can be found:

$$T_{fl} = \frac{1 - k_t}{2} T \quad (14)$$

$$T_{fr} = \frac{1 - k_t}{2} T \quad (15)$$

$$T_{rl} = \frac{k_t}{2} T + k_d \Delta_\omega \quad (16)$$

$$T_{rr} = \frac{k_t}{2} T - k_d \Delta_\omega \quad (17)$$

where  $k_d$  is the viscous differential constant and  $\Delta_\omega$  is difference in rear wheel speed; i.e.,  $\Delta_\omega = \omega_{rl} - \omega_{rr}$ .

### 3.1.2. Aerodynamics

A simple aerodynamic model is used to capture the speed dependent down force ( $F_{az}$ ) and drag ( $F_{ax}$ ) quantities acting on the vehicle. These forces are applied to the vehicle center of pressure shown in Figure 1. Other aerodynamic affects such as yaw and pitch are coupling are neglected for the purposes of this work. The aerodynamic forces are described by:

$$F_{az} = \frac{1}{2} C_L \rho A v_x^2 \quad (18)$$

$$F_{ax} = \frac{1}{2} C_D \rho A v_x^2 \quad (19)$$

The constants  $C_L$ , and  $C_D$  are the downforce and drag coefficients, respectively. The vehicle's frontal area is denoted with  $A$  and the air density is denoted with  $\rho$ .

### 3.1.3. Load Transfer

The normal tire load is calculated by summing the forces and moments about the body fixed-coordinates seen in Figure 1 and enforcing a roll stiffness distribution  $D \in [0, 1]$  such that the front axle load transfer is a fixed proportion of the total load transfer. This yields the following linear system to be solved:

$$\begin{bmatrix} 1 & 1 & 1 & 1 \\ -w_f & w_f & -w_r & w_r \\ -a & -a & b & b \\ D-1 & 1 & -D & -D \end{bmatrix} \begin{bmatrix} Fz_{fl} \\ Fz_{rl} \\ Fz_{rl} \\ Fz_{rr} \end{bmatrix} = \begin{bmatrix} -mg - F_{az} \\ -hF_y \\ (a_a - a)F_{az} + hF_x \\ 0 \end{bmatrix} \quad (20)$$

### 3.1.4. Tires

The tire's friction forces are calculated via an empirical formula that responds to changes in loads, lateral slip angle, and longitudinal slip. It is based on the simplified Pacejka tire model presented in [59, 66]. The slip ratio ( $\kappa$ ) and slip angle ( $\alpha$ ) are calculated:

$$\kappa = - \left( 1 + \frac{R\omega}{v_{xtire}} \right) \quad (21)$$

and,

$$\alpha = - \arctan \left( \frac{v_{ytire}}{v_{xtire}} \right) \quad (22)$$

where  $R$  is the effective rolling radius of the tire and  $v_{xtire}$ ,  $v_{ytire}$  are the longitudinal and lateral velocities of the tire accounting for vehicle rotation. A detail description of the adopted tire model can be found in [59, 66].

### 3.1.5. Path Intrinsic Coordinate System

In order to facilitate a convenient mechanism for constraining the vehicle to stay within the track bounds, path intrinsic coordinates will be used. This coordinate system models the vehicle trajectory with respect to the road centerline. It is depicted in Figure 2. The heading angle deviation ( $e_\psi$ ) represents the difference between the path heading and the vehicle heading angle while the lateral deviation ( $e_y$ ) refers to the vehicle lateral deviation from the path centerline. The vehicle speed in the path reference frame is denoted as  $\dot{s}$ . The quantities  $\dot{s}$ ,  $e_\psi$ , and  $e_y$  are calculated as follows:

$$\dot{s} = \frac{v_x \cos(e_\psi) - v_y \sin(e_\psi)}{1 - e_y C} \quad (23)$$

where  $C$  is the path curvature and a known function of path distance i.e.,  $C = C(s)$ .

$$\dot{e}_\psi = \dot{\psi} - C\dot{s} \quad (24)$$

$$\dot{e}_y = v_x \sin(e_\psi) + v_y \cos(e_\psi) \quad (25)$$

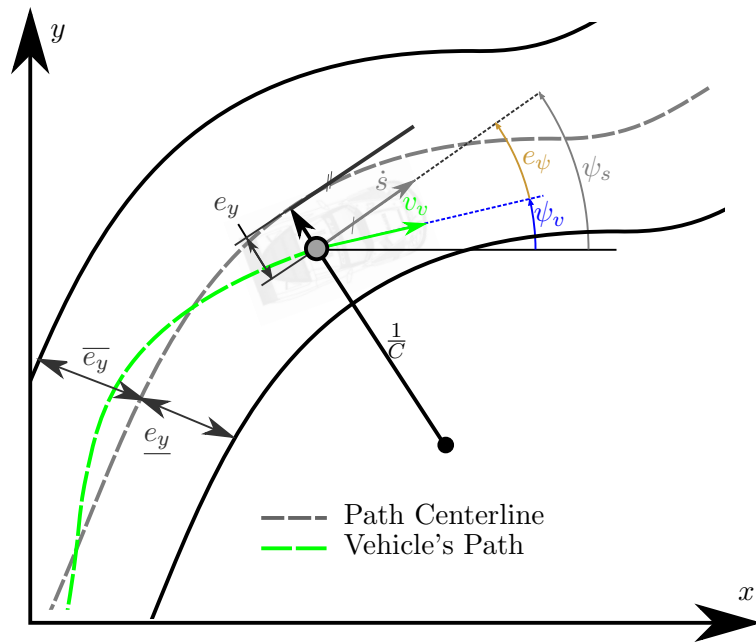


Figure 2. Path intrinsic coordinate description. Note subscripts  $s$  and  $v$  refer to the path and vehicle frame respectively.

### 3.1.6. Distance Based Description

The full system description can now be written as:

$$\dot{\mathbf{x}} = f(\mathbf{x}, \mathbf{u}, t) \quad (26)$$

where,

$$\mathbf{x} = [e_\psi \ e_y \ v_x \ v_y \ \psi \ \omega_p \ \delta \ T]^T \quad (27)$$

The last step is to convert the independent variable from time to space. This is done to eliminate the free final time boundary condition that arises if the system is posed in the time domain. Once converted, the final distance is fixed; thus, the free final boundary condition is eliminated. This transformation is achieved via application of the chain rule of differentiation to the system dynamics in: (26).

$$\frac{d\mathbf{x}}{dt} \frac{dt}{ds} = \frac{d\mathbf{x}}{ds} = \frac{\dot{\mathbf{x}}}{\dot{s}} \quad (28)$$

## 3.2. Cascaded Optimization

In this section, the proposed cascaded optimization approach will be detailed. This optimization structure is comprised of a lower level controller which utilizes a variable cost MPC to drive the vehicle around the track while minimizing the cost function at each MPC preview horizon. The variable cost allows the controller in a local horizon to blend two different objectives: minimizing time or maximizing exit velocity at the end of the horizon.

### 3.2.1. Inner Loop MPC

This loop is responsible for solving the optimal set of vehicle controls  $u_1$  and  $u_2$  over the prescribed maneuver while minimizing a cost function in each preview horizon. This Model Predictive Control (MPC) strategy utilizes a moving horizon where a portion of the track is previewed and an optimal control problem is solved over this portion. The horizon then moves forward and the process repeats around the track. Within in each horizon the optimal control problem can be posed as:

$$\begin{aligned} \min_u \quad & J(x, x(s), u(s), w_k) = J_{MPC} \\ \text{s.t.} \quad & \frac{dx}{ds} - f(s, x(s), u(s)) = 0 \\ & h(s, x(s), u(s)) \leq 0 \\ & g_b(x(s_0), x(s_f), u(s_0), u(s_f)) = 0 \end{aligned} \quad (29)$$

where  $J$  is a general cost-functional that will be further clarified in the proceeding discussion. The function  $f(\cdot) \in \mathbb{R}^n$  represents the system dynamics described by (28). The function  $g(\cdot) \in \mathbb{R}^{n_g}$  is used to constrain the lateral deviation of the vehicle to stay within the track width boundaries ( $\underline{e}_y \leq e_y \leq \bar{e}_y$ ) and to limit the maximum engine power ( $P_{eng} = T\omega_{rear} \leq P_{eng}^{max}$ ). The function  $g_b(\cdot) \in \mathbb{R}^{n_{g_b}}$  captures boundary conditions of the problem.

In the cascaded optimization formulation, a mixed-cost function capable of blending the objectives of minimizing the local segment maneuvering time and exit velocity will be used. The two objectives are balanced via the weighting terms  $w_k$ , where the subscript  $k \in \{t, v_x\}$  denotes either time or longitudinal velocity. Therefore, the local MPC cost function used in each horizon can be written as:

$$J_{MPC}^i(Z^i) = \underbrace{w_t^i \left( \frac{t(s_{horizon}^i)}{s_t} \right)^2}_{\text{Minimize Time}} - \underbrace{w_{v_x}^i \left( \frac{v_x(s_{horizon}^i)}{s_{v_x}} \right)^2}_{\text{Maximize Exit Velocity}} \quad (30)$$

In this cost structure, proper scaling between the objectives is handled via the scaling (normalization) terms. These are denoted  $s_t$  and  $s_{v_x}$  and are, respectively, the maximum values of time and velocity found in the reference time-optimal MPC solution (see section 3.3). Their values are fixed throughout the whole maneuver.

The computation process given a global set of weights  $\mathbf{Z}$  is depicted in Figure 3. First, the problem domain  $s \in [s_0, s_f]$  is divided in to  $i = 1, 2, \dots, N$  segments. These segments define the MPC update interval:  $s_{MPC} = (s_f - s_0)/N$ . Next, the first MPC horizon ① is posed over the horizon  $s^1 \in [s_0^1 = s_0, s_0^1 + s_{horizon}]$  with initial conditions  $x_0^1 = x_0$ . The preview horizon ( $s_{horizon}$ ) is a chosen parameter and can be seen in Table A2. Now, the optimal control problem (29) can be solved over this horizon using the local cost  $J^1(Z^1) = (30)$ . Where the weights  $Z^1 = [w_t^1 \ w_{v_x}^1]$  blend the objectives minimizing time and maximizing velocity over this horizon. Once this optimal control problem is solved, the global solution is then updated over the MPC update interval ②. Next, the problem advances forward by the MPC update interval and the next MPC horizon is formed ③. This next segment starts at  $s_0^2 = s_0^1 + s_{MPC}$  and has the initial conditions  $x_0^2 = x^1(s_0^2)$  are found from the previous horizon ④. The second horizon is then solved and the process is repeated around the entire racing circuit for all  $i = 1, 2, \dots, N - 1$  MPC horizons. To allow the vehicle to come up to operating speed, the maneuver timing is started a distance after the initial simulation distance  $s_0$  which is denoted as  $s_{start}$ . This simulates the ‘out lap’ a human driver performs when first going on a racing circuit and comes up to speed

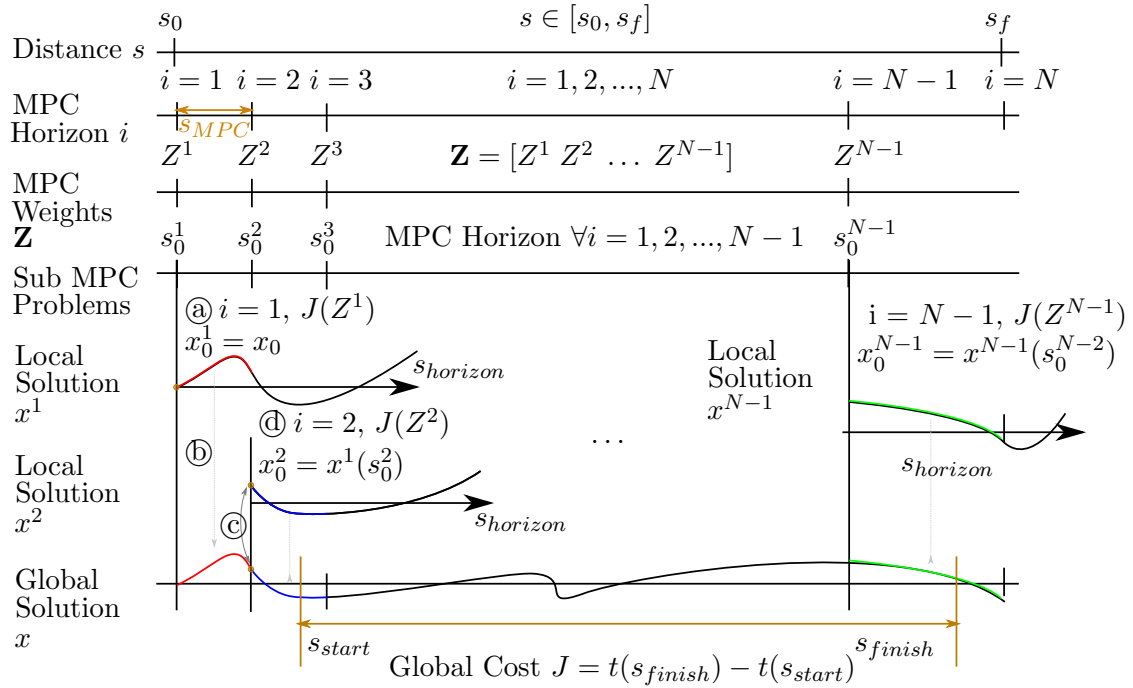


Figure 3. MPC Lap Simulation.

before the timed maneuver begins. Similarly, an ‘in lap’ is also simulated as the timed portion of the maneuver ( $s_{finish} - s_{start}$ ) occurs before the simulation is complete at distance  $s_f$ . Therefore, the global performance index is:  $J = t(s_{finish}) - t(s_{start})$ .

### 3.2.2. Outer Loop Optimization

The objective of the outer loop optimization is to find the optimal set of weights that the inner loop controller will use in each local MPC horizon such that the global maneuvering time ( $t(s_{end}) - t(s_{start})$ ) is minimized. The cascaded optimization can be written as:

$$\begin{array}{l}
 \min_{\mathbf{Z}} \quad J = t(s_{end}) - t(s_{start}) \\
 \text{Sub MPC Problem: } \text{for } i = 1, 2, \dots, N - 1 \\
 \text{Optimal Control Problem (29)} \\
 \text{s.t.} \quad \begin{array}{l}
 s^i \in [s_o^i (s_o^i + s_{horizon})] \\
 s^{i+1} = s_o^i + \frac{(s_f - s_o)}{N} \\
 x_0^{i+1} = x(s^{i+1}) \\
 w_k^i \in [0, 1]
 \end{array}
 \end{array} \quad (31)$$

where  $\mathbf{Z}$ , the decision variable of the outer loop and contains the set of weights ( $w_k^i$ ,  $k \in \{t, v_x\}$ ) to be used over each local MPC horizon. In other words:

$$\mathbf{Z} = [Z^1 \ Z^2 \ \dots \ Z^{N-1}]^T = [w_t^1 \ w_{v_x}^1 | w_t^2 \ w_{v_x}^2 | \dots | w_t^{N-1} \ w_{v_x}^{N-1}]^T \quad (32)$$

where N-1 is the number of MPC segments on the track. Therefore, the global set of weights  $\mathbf{Z} \in \mathbb{R}^{2(N-1) \times 1}$ . Furthermore, each element of  $\mathbf{Z}$  is constrained such that  $w_k^i \in$

[0, 1].

Note that as will be highlighted below, the cascaded optimization is generally non-convex with substantial computational overhead. We applied genetic algorithms and used supercomputing clusters to arrive at the results presented below.

### 3.3. Reference Time-Optimal MPC Solution

To facilitate comparison between the cascaded optimization approach, we will consider a traditional fixed-cost time-optimal MPC applied over the whole maneuver. The local cost function for this time-optimal MPC is:

$$J_t^i = \int_{s_0^i}^{s_{horizon}^i} \frac{1}{\dot{s}} ds \quad (33)$$

Hereafter, we refer to the solution to this formulation as reference time-optimal MPC solution.

## 4. Results and Discussion

In this section, the preceding control strategies are applied to two racing circuits: Hockenheim and Nürburgring. On each racing circuit, the globally optimized MPC will be compared to the traditional fixed-cost time-optimal MPC. The vehicle used in this work is representative of a Formula 1 racing car and was presented in [59, 66]. The parameters used can be found in Table A1 in the Appendix. To solve the problem posed in (31), two solvers were utilized. For the outer loop optimization, the genetic algorithm from MATLAB's global optimization tool box [71] was employed to find the global set of weights  $\mathbf{Z}$  that minimize global maneuvering time. A genetic algorithm was chosen as there are many local optima in the solution space (which will be further discussed later). The inner loop performs the MPC procedure outlined in Figure 3 and recursively solves the optimal control problem described in (29). The solutions for these optimal control problems are found via an orthogonal collocation method (implemented in the software package GPOPS-II [72]). The MPC algorithm and simulation parameters can be seen in Table A2 in the Appendix.

### 4.1. Hockenheim

This race course is located in the town of Hockenheim, Germany and was open in 1932 [73]. In this research, the short configuration will be used which consists of a 2.6km closed road course with 10 various radii corners. The globally optimized MPC and traditional time-optimal MPC trajectories can be seen in Figure 4. The trajectories are quite similar over most of the race course with one very large difference occurring from the apex to exit of turn four. The key data channels from this simulation can be seen in Figure 5. The top plot in this figure is the vehicle's longitudinal velocity over the lap and right below is the split velocity. Split channels provide a convenient means for comparing these two solutions and are defined here as the difference between the two simulations at each distance on the track. Formally written:

$$\Delta y = y(s)|_{timeOpt} - y(s)|_{locallyOptMPC} \quad (34)$$

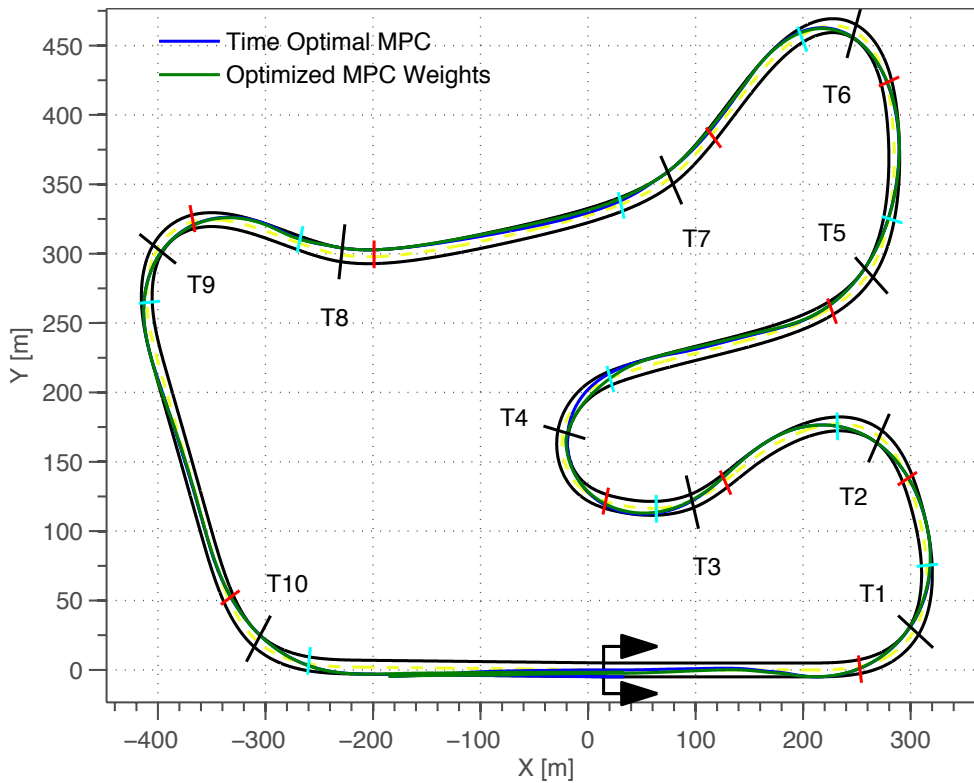


Figure 4. Trajectories on the Hockenheim racing circuit. Numbers with the prefix ‘T’ denote the 10 different turn apexes on the course. Red waylines denote corner entry locations and cyan lines denote corner exit lines.

where  $y$  can be any measured state, control input, or calculated channel. The split velocity trace in Figure 5 shows that adjusting speed by just a few m/s in certain sections can have an impact on the final performance. The third plot of Figure 5 shows the split-time plot and is the key indicator for showing the advantage of the globally optimized MPC. The reader can see that right after the apex of turn four through corner exit and all the way to the entry of turn 6 (to a lesser degree) that the slope of the globally optimized MPC  $\Delta t$  is down; i.e., this solution is gaining time on the reference time-optimal MPC solution. Thus, at the same location on the track, there has been less elapsed time with the globally optimized MPC. Turn four is the key location on the circuit where the global weights were able to change the trajectory to yield a net benefit. The controller did this by sacrificing time right before the apex of turn four as can be seen on the same plot (where the  $\Delta t$  traces is increasing to a peak right past the turn four apex). This is the key point demonstrating how the globally optimized MPC mimics a human driver, it can learn to sacrifice time in a particular location of the track, in this case the entry of turn four through the apex, in order to ‘setup’ the next section with higher velocity and ultimately achieve a better solution over entire maneuver. The fourth plot in this figure shows the split ( $\Delta e_y$ ) racing line and again, the key difference between the two solution is at turn four where the globally optimized MPC is able to apex the turn earlier, sacrificing some time early in the corner while achieving a higher velocity at corner exit.

The globally optimized weights themselves are quite noisy as can be seen in the last trace of Figure 5 and overlaid on the track map in Figure 6. Much of this noise comes

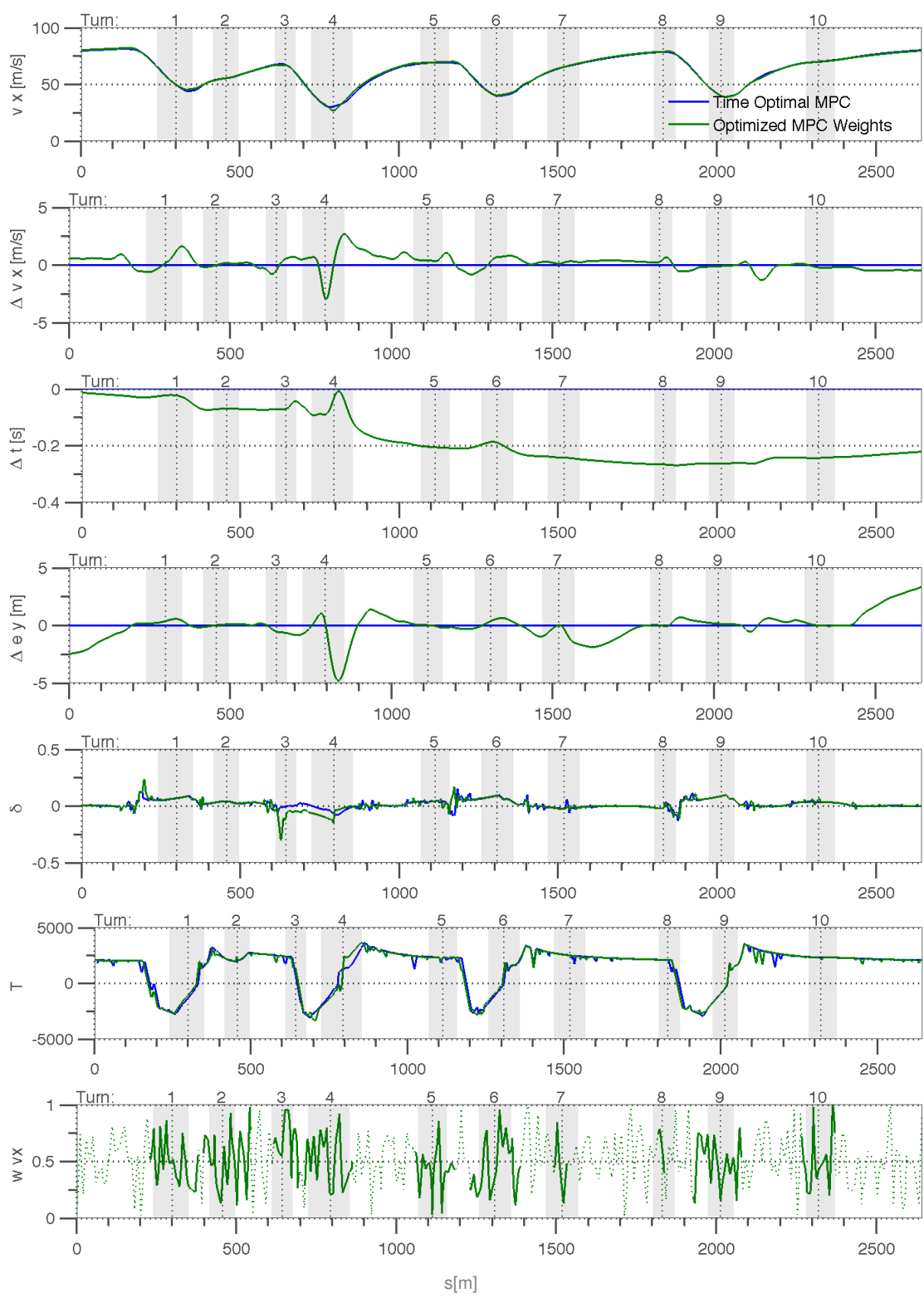


Figure 5. Hockenheim distance histories. Blue denotes the reference time optimal MPC and green is the optimized cascaded optimization. From top to bottom longitudinal velocity, split velocity, split time, split racing line, steering wheel angle, torque demand, and contribution of the exit velocity MPC weight in each local segment. The weight contribution is defined as:  $w_{v_x} / (w_t + w_{v_x})$ . Weights in straight portions of the track are dotted to emphasize results during corners. Note that each turn is denoted with a grey patch and corner entry and exit points correspond to those denoted in Figure 4. Corner apex location makeup the  $x$  grid location in these plot and corner number are located at the top of each channel.

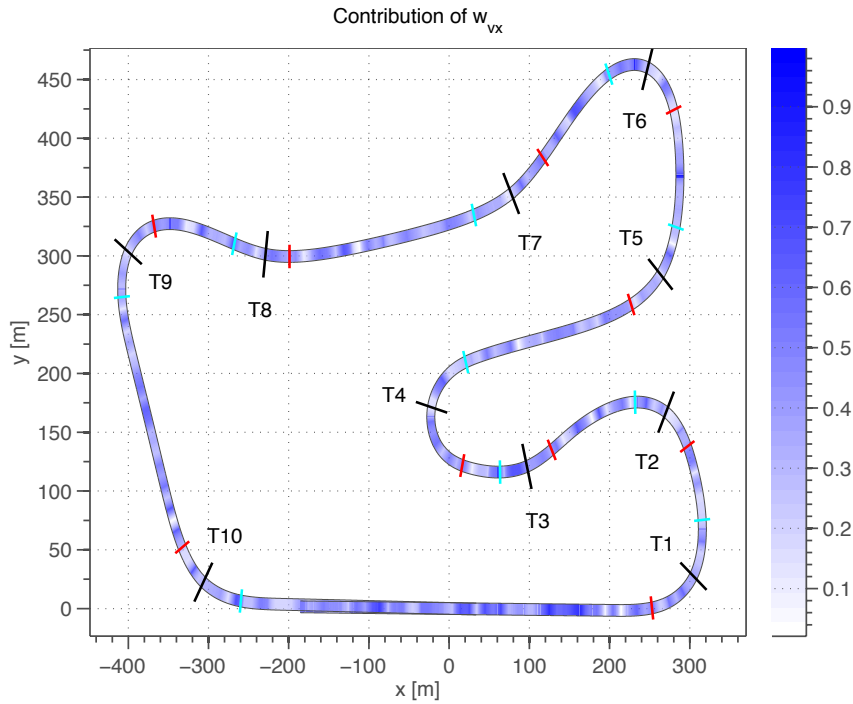


Figure 6. Contribution of the exit velocity MPC weight in each local segment. This contribution is defined as:  $w_{v_x}/(w_t + w_{v_x})$ .

from the fact that when traveling in a straight line, the objectives of maximizing velocity and minimizing time are nearly identical. This is demonstrated in the control quantities: steering ( $\delta$ ) and torque demand ( $T$ ) shown in Figure 5. On the straight sections of track (section without highlights denoting the corners), the control quantities of the globally optimal MPC are nearly identical to the time-optimal MPC in spite of the fact that the globally optimal MPC is choosing different values for the contribution of exit velocity and maneuvering time at each local segment. The key benefit to this structure is that the weights can change in a corner to setup different trajectories that could impact global performance. There is a small section of track right after the apex of turn four where the globally optimal MPC more heavily weights the exit velocity ( $w_{v_x}$ ) and the trajectory in that location is able to change enough to setup the next section of track yielding a better maneuvering time overall. The final results can be seen in Table 1.

#### 4.2. Nürburgring

The two control strategies were also applied to the Nürburgring race course. This is a very historic track located in the town of Nurburg Germany and was constructed in the 1920s [74]. For the purposes of this work, the grand prix configuration consisting of 14 turns over a distance of 4.5km was used. The vehicle trajectories can be seen in Figure 7. The results on this track were very similar to Hockenheim; there was one key location from the apex of turn six (T6) to corner exit that comprised much of the performance advantage of the globally optimized MPC. The distance histories of velocity, split velocity, split time, split racing line, steering wheel angle, torque demand, and contribution of exit velocity weight can be seen in Figure 8. Just as in the Hockenheim case, changing speed by just a few m/s in key locations around the course yields global performance benefits.

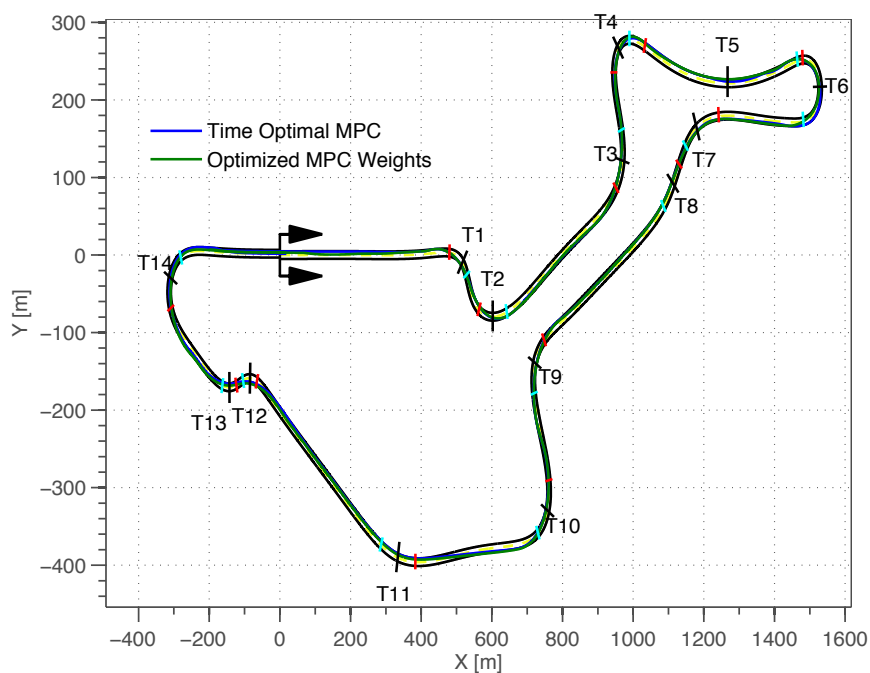


Figure 7. Trajectories on the Nürburgring racing circuit. Numbers with prefix ‘T’ denote corner apexes, red waylines denote corner entry locations and cyan lines denote corner exit lines.

Looking at the split time ( $\Delta t$ ) plot shows that the majority of the performance advantage of the globally optimized MPC comes just after the apex of turn six to just after corner exit. The globally optimal trajectory sacrifices time just before the apex of turn six to take advantages of higher speed all the way to the entry of turn nine (T9) yielding a net improvement. The split racing line plot ( $\Delta e_y$ ) shows that a very different racing line is used in this turn.

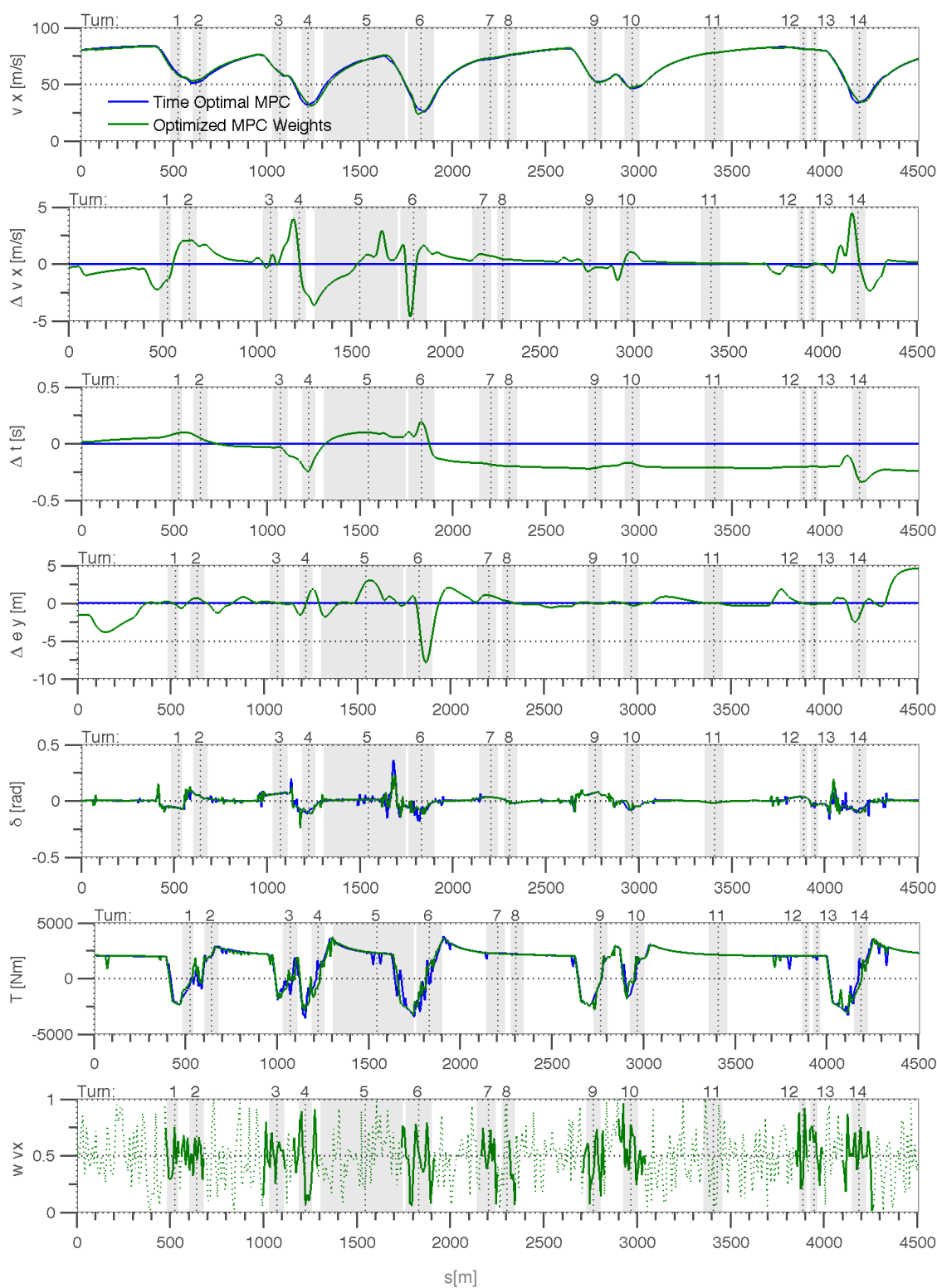


Figure 8. Nürburgring distance histories. Blue denotes the reference time optimal MPC and green is the optimized cascaded optimization. From top to bottom longitudinal velocity, split velocity, split time, split racing line, steering wheel angle, torque demand, and contribution of the exit velocity MPC weight in each local segment. The weight contribution is defined as:  $w_{v_x}/(w_t + w_{v_x})$ . Weights in straight portions of the track are dotted to emphasize results during corners. Note that each turn is denoted with a grey patch and corner entry and exit points correspond to those denoted in Figure 7. Corner apex location makeup the  $x$  grid location in these plot and corner number are located at the top of each channel.

Table 1. Results from Hockenheim and Nürburgring.

Course	Controller	Maneuvering		Performance	
		Time [s]	$\Delta$ Time [s]	$\Delta$ [%]	
Hockenheim	Time optimal MPC	44.471	-	-	
	Globally optimized MPC	44.264	-0.207	-0.466	
Nürburgring	Time optimal MPC	72.121	-	-	
	Globally optimized MPC	71.866	-0.255	-0.354	

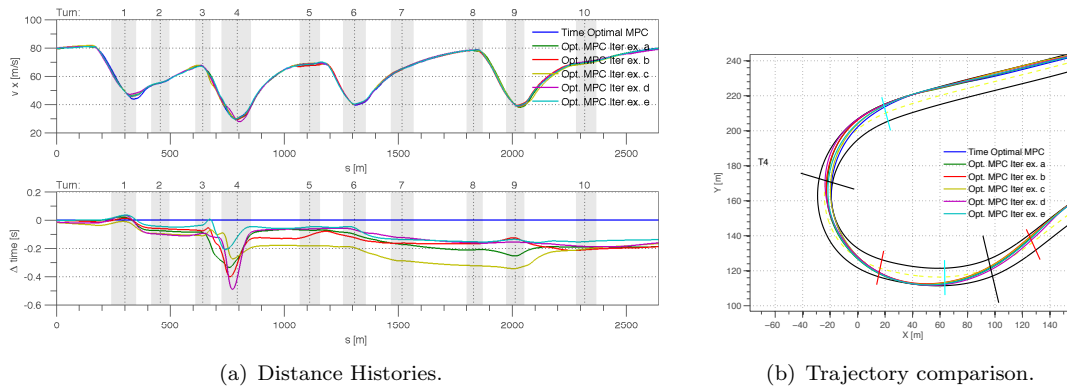


Figure 9. Five example iterate solutions show outperformance of the time optimal MPC.

### 4.3. Summary of Results and Discussion

The final performance of both controllers can be seen in Table 1. While these performance gains may seem small to the casual observer, in the context of motorsports these can be significant. In Formula 1 racing, teams spend millions of dollars for millisecond gains in lap time performance [34, 75]. Moreover, these small gains come with dramatic changes to the racing line. This corroborates the authors’ experiences with professional drivers. Different drivers are able to achieve similar performance with a very different trajectory or driving style. Mathematically speaking, this demonstrates the existence of multiple local minima in the solution space, a point which has not been directly discussed in reviewed literature. It is the opinion of the authors that these local minima could be used to explain different driving styles that are exhibited by professional drivers. To further support this point, five other iterates of the genetic algorithm outputs for the global weight ( $\mathbf{Z}$ ) search are plotted for the Hockenheim track in Figure 9. Their respective maneuvering times and improvement over the time-optimal MPC can be seen in Table 2. It is clear to see that this notion of globally optimizing the local MPC weights has advantage over the traditional fixed cost time optimal MPC and is able to outperform it repeatably. Moreover, there are many different sets of weights that all out perform the time optimal MPC and thus demonstrating the existence of multiple local minima in the solution space.

## 5. Conclusions

In this paper, a cascaded optimization structure is formulated to model how a professional driver is able to optimize over local segments of race circuits to minimize maneuvering time over the whole track. An inner loop MPC with a variable cost function is used to set local control and an outer loop optimization searches to find the best set of weights that

Table 2. Other iterates on Hockenheim showing globally optimized MPC outperforming time optimal MPC.

Controller	Maneuvering Time [s]	$\Delta$ Time [s]	Performance $\Delta$ [%]
Time optimal MPC	44.471	-	-
Example iterate a	44.286	-0.185	-0.416
Example iterate b	44.286	-0.185	-0.415
Example iterate c	44.323	-0.148	-0.334
Example iterate d	44.325	-0.146	-0.328
Example iterate e	44.335	-0.136	-0.306

the inner loop will use in each horizon to optimally blend the objectives of minimizing time or maximizing velocity in each MPC horizon. This cascaded optimization structure is then used to simulate a Formula 1 car on two well-known race courses: Hockenheim and Nürburgring. The results are compared to a traditional fixed-cost time-optimal MPC controller. In both cases, the cascaded optimization is able to outperform the time-optimal controller. Moreover, examining other iterates in the solution space demonstrates that there are several different solutions with similar performance; i.e., a demonstration of the existence of local minima in solution space. The later is a corroboration of the intuition and practical field observations that different driving styles may achieve very similar maneuvering times. Future work will look at exploiting this optimization structure to further analyze the driving style differences between different human drivers.

## Acknowledgement

The authors acknowledge the acknowledged for a generous allotment of compute time on the Palmetto Supercomputing Cluster at Clemson University.

## References

- [1] Wright P, Matthews T. Formula 1 technology. SAE Technical Paper; 2001. Report no.:
- [2] Casanova D. On minimum time vehicle manoeuvring: The theoretical optimal lap [dissertation]. Cranfield University; 2000.
- [3] Sharp R, Peng H. Vehicle dynamics applications of optimal control theory. *Vehicle System Dynamics*. 2011 July;49(7):1073–1111.
- [4] Maniowski M. Optimisation of driver actions in rwd race car including tyre thermodynamics. *Vehicle System Dynamics*. 2016;54(4):526–544.
- [5] Anderson JR, Ayalew B, Weiskircher T. Modeling a professional driver in ultra-high performance maneuvers with a hybrid cost MPC. In: American Control Conference (ACC), 2016; July. Boston Marriott Copley Place, Boston, MA, USA: IEEE; 2016. p. 1981–1986.
- [6] Kelly D, Sharp R. Time-optimal control of the race car: a numerical method to emulate the ideal driver. *Vehicle System Dynamics*. 2010;48(12):1461–1474.
- [7] Milliken WF, Milliken DL, et al. Race car vehicle dynamics. Vol. 400. Society of Automotive Engineers Warrendale; 1995.
- [8] Scherenberg H. Mercedes-benz racing design and cars experience. SAE Technical Paper; 1958. Report No.: 580042.
- [9] Griffiths R. Minimum time simulation of a racing car [master’s thesis]. School of Mechanical Engineering, Cranfield University; 1992.
- [10] Dominy R. Aerodynamic influences on the performance of the grand prix racing car. *Proceedings of the Institution of Mechanical Engineers, Part D: Journal of Automobile Engineering*. 1984;198(2):87–93.
- [11] Brayshaw D, Harrison M. A quasi steady state approach to race car lap simulation in order to

- understand the effects of racing line and centre of gravity location. *Proceedings of the Institution of Mechanical Engineers, Part D: Journal of Automobile Engineering*. 2005;219(6):725–739.
- [12] Tremlett A, Assadian F, Purdy D, Vaughan N, Moore A, Halley M. Quasi-steady-state linearisation of the racing vehicle acceleration envelope: a limited slip differential example. *Vehicle System Dynamics*. 2014;52(11):1416–1442.
- [13] Kapania NR, Subosits J, Gerdes JC. A sequential two-step algorithm for fast generation of vehicle racing trajectories. *Journal of Dynamic Systems, Measurement, and Control*. 2016;138(9):091005.
- [14] Weir DH, McRuer DT. A theory for driver steering control of motor vehicles; 1968. Report No.: HS-005 311.
- [15] Rix J, Cole D. Models of human learning applicable to the vehicle steering task. In: *Proceedings of the 6th International Symposium on Advanced Vehicle Control*. International Conference Center, Hiroshima, Japan; 2002. p. 683–688.
- [16] Sharp R, Casanova D, Symonds P. A mathematical model for driver steering control, with design, tuning and performance results. *Vehicle System Dynamics: International Journal of Vehicle Mechanics and Mobility*. 2000;33(5):289–326.
- [17] MacAdam CC. Application of an optimal preview control for simulation of closed-loop automobile driving. *IEEE Transactions on Systems, Man and Cybernetics*. 1981 June;11(6):393–399.
- [18] The VehicleSim steer controller. *Mechanical Simulation*; 2011. Report no.:
- [19] Guo K, Guan H. Modelling of driver/vehicle directional control system. *Vehicle System Dynamics*. 1993;22:141–184.
- [20] Macadam CC. Understanding and modeling the human driver. *Vehicle System Dynamics: International Journal of Vehicle Mechanics and Mobility*. 2003;40(1-3):101–134.
- [21] Plöchl M, Edelmann J. Driver models in automobile dynamics application. *Vehicle System Dynamics*. 2007;45(7-8):699–741.
- [22] Rievily R, Minaker B, Maurini M, Shallavari I, Laport J. Development of an advanced driver model and simulation for automotive racing. *SAE*. 2009;01(0434).
- [23] Braghin F, Cheli F, Melzi S, Sabbioni E. Race driver model. *Computers and Structures*. 2008; 86:1503–1516.
- [24] Botta M, Gautieri V, Loiacono D, Lanzi PL. Evolving the optimal racing line in a high-end racing game. In: *2012 IEEE Conference on Computational Intelligence and Games (CIG)*; September. Granada, Spain: IEEE; 2012. p. 108–115.
- [25] Cardamone L, Loiacono D, Lanzi PL, Bardelli AP. Searching for the optimal racing line using genetic algorithms. In: *Togelius GNYJ, editor. Computational Intelligence and Games (CIG), 2010 IEEE Symposium on*; August. IT University of Copenhagen, Center for Computer Games Research, Copenhagen, Denmark: IEEE; 2010. p. 388–394.
- [26] Lepetic M, Klancar G, Skrjanc I, Matko D, Potocnik B. Time optimal path planning considering acceleration limits. *Robotics and Autonomous Systems*. 2003;45(3):199–210.
- [27] Velenis E, Tsiotras P. Optimal velocity profile generation for given acceleration limits: Theoretical analysis. In: *American Control Conference*; June 8-10. Portland, OR: IEEE; 2005. p. 1478–1483.
- [28] Velenis E, Tsiotras P. Optimal velocity profile generation for given acceleration limits; the half-car model case. In: *2005 IEEE International Symposium on Industrial Electronics*; December. Dubrovnik, Croatia; 2005. p. 355–360.
- [29] Lipp T, Boyd S. Minimum-time speed optimization over a fixed path. *International Journal of Control*. 2014;1(1):1–15.
- [30] Verschuer D, Demeulenaere B, Swevers J, De Schutter J, Diehl M. Time-optimal path tracking for robots: A convex optimization approach. *Automatic Control, IEEE Transactions on*. 2009; 10(54):2318–2327.
- [31] Fujioka T, Kimura T. Numerical simulation of minimum-time cornering behavior. *JSAE Review*. 1992;13(1).
- [32] Hendrikx J, Meijlink J, Kriens R. Application of optimal control theory to inverse simulation of car handling. *Vehicle System Dynamics*. 1996;26:449–461.
- [33] Cossalter V, Da Lio M, Lot R, Fabbri L. A general method for the evaluation of vehicle manoeuvrability with special emphasis on motorcycles. *Vehicle system dynamics*. 1999;31(2):113–135.
- [34] Limebeer DJ, Rao AV. Faster, higher and greener: Vehicular optimal control. *IEEE Control Systems Magazine*. 2015 April;:37–56.
- [35] Bertolazzi E, Biral F, Da Lio M. Symbolic-numeric indirect method for solving optimal control problems for large multibody systems. *Multibody System Dynamics*. 2005;13(2):233–252.
- [36] Tremlett A, Massaro M, Purdy D, Velenis E, Assadian F, Moore A, Halley M. Optimal control of motorsport differentials. *Vehicle System Dynamics*. 2015;53(12):1771–1794.

- [37] Maggio F, Biral F, Da Lio M. How gearbox ratios influence lap time and driving style. an analysis based on time-optimal maneuvers. SAE Technical Paper; 2003. Report No.: 2003-32-0056.
- [38] Simon B, Vittore C, Matteo M, Martino P. Application of the “optimal maneuver method” for enhancing racing motorcycle performance. SAE International Journal of Passenger Cars-Mechanical Systems. 2008;1(2008-01-2965):1311–1318.
- [39] Lot R, Dal Bianco N. Lap time optimisation of a racing go-kart. *Vehicle System Dynamics*. 2015; 52(2):210–230.
- [40] Lot R, Dal Bianco N. The significance of high-order dynamics in lap time simulations. In: IAVSD 2015: 24th International Symposium on Dynamics of Vehicles on Roads and Tracks; August. Graz, AT: CRC Press; 2015.
- [41] Tavernini D, Massaro M, Velenis E, Katzourakis DI, Lot R. Minimum time cornering: the effect of road surface and car transmission layout. *Vehicle System Dynamics*. 2013;51(10):1533–1547.
- [42] Betts JT. Practical methods for optimal control and estimation using nonlinear programming. Vol. 19. Warrendale, PA: Siam; 2010.
- [43] Betts JT. Survey of numerical methods for trajectory optimization. *Journal of guidance, control, and dynamics*. 1998;21(2):193–207.
- [44] Allen J. Computer optimization of cornering line [master’s thesis]. Cranfield University; 1997.
- [45] Casanova D, Sharp R. Minimum time manoeuvring: The significance of yaw inertia. *Vehicle System Dynamics*. 2000;34(34):77–115.
- [46] Casanova D, Sharp R, Symonds P. Sensitivity to mass variations of the fastest possible lap of a formula one car. *Vehicle System Dynamics Supplement*. 2001;35(35):119–134.
- [47] Casanova D, Sharp R, Symonds P. On the optimisation of the longitudinal location of the mass centre of a formula one car for two circuits. In: Proceedings of the 6th International Symposium on Automotive Control (AVEC 2002); September 9–13; Vol. 2. Citeseer; Japan, Hiroshima: SAE; 2002. p. 6–12.
- [48] Masouleh MI, Limebeer DJ. Heave spring and ride height optimisation of a formula one car suspension system. In: Takai S, editor. 2015 54th IEEE Conference on Decision and Control (CDC); December. Osaka, Japan: IEEE; 2015. p. 165–170.
- [49] Garg D, Patterson M, Hager WW, Rao AV, Benson DA, Huntington GT. A unified framework for the numerical solution of optimal control problems using pseudospectral methods. *Automatica*. 2010;46(11):1843–1851.
- [50] Berntorp K, Olofsson B, Bernhardsson B, Lundahl K, Nielsen L. Models and methodology for optimal vehicle maneuvers applied to a hairpin turn. In: American Control Conference (ACC), 2013; June. Renaissance Washington, DC Downtown Hotel, Washington, DC: IEEE; 2013. p. 2139–2146.
- [51] Berntorp K, Olofsson B, Lundahl K, Nielsen L. Models and methodology for optimal trajectory generation in safety-critical road–vehicle manoeuvres. *Vehicle System Dynamics*. 2014;:1–29.
- [52] Lundahl K, Berntorp K, Olofsson B, Åslund J, Nielsen L. Studying the influence of roll and pitch dynamics in optimal road-vehicle maneuvers. In: 23rd International Symposium on Dynamics of Vehicles on Roads and Tracks; August. Qingdao, China; 2013.
- [53] Sharp R. A method for predicting minimum-time capability of a motorcycle on a racing circuit. *Journal of Dynamic Systems, Measurement, and Control*. 2014;136(4):041007.
- [54] Cossalter V, Lot R, Tavernini D. Optimization of the centre of mass position of a racing motorcycle in dry and wet track by means of the “optimal maneuver method”. In: Pipeleers G, editor. Mechatronics (ICM), 2013 IEEE International Conference on; February. Department of Management and Engineering, University of Pado, Vicenza, VI, Italy: IEEE; 2013. p. 412–417.
- [55] Kelly D, Sharp R. Time-optimal control of the race car: influence of a thermodynamic tyre model. *Vehicle System Dynamics*. 2012 April;50(4):641–662.
- [56] Tremlett A, Limebeer D. Optimal tyre usage for a formula one car. *Vehicle System Dynamics*. 2016; 54(10):1448–1473.
- [57] Limebeer D, Perantoni G, Rao A. Optimal control of formula one car energy recovery systems. *International Journal of Control*. 2014;87(10):2065–2080.
- [58] de Castro R, Tanelli M, Araujo RE, Savaresi SM. Minimum-time manoeuvring in electric vehicles with four wheel-individual-motors. *Vehicle System Dynamics: International Journal of Vehicle Mechanics and Mobility*. 2014;52(6):824–846.
- [59] Perantoni G, Limebeer DJ. Optimal control for a formula one car with variable parameters. *Vehicle System Dynamics*. 2014;52(5):653–678.
- [60] Limebeer D, Perantoni G. Optimal control of a formula one car on a three-dimensional track—part 2: Optimal control. *Journal of Dynamic Systems, Measurement, and Control*. 2015;137(5):051019.
- [61] Verschueren R, De Bruyne S, Zanon M, Frasch JV, Diehl M. Towards time-optimal race car driving

- using nonlinear mpc in real-time. In: 53rd IEEE Conference on Decision and Control; December. J.W. Marriott Hotel, Los Angeles, CA, USA: IEEE; 2014. p. 2505–2510.
- [62] Pesch H, Gerdts M. Simulation of test-drivers of automobiles at driving limit. In: Jäger W, Krebs HJ, editors. Mathematics—key technology for the future. Berlin, Germany: Springer; 2003. p. 74–83.
- [63] Gerdts M. A moving horizon technique for the simulation of automobile test-drives. ZAMM-Journal of Applied Mathematics and Mechanics. 2003;83(3):147–162.
- [64] Gerdts M, Karrenberg S. Generating locally optimal trajectories for an automatically driven car. Optimization and Engineering. 2009;10(4):439–463.
- [65] Prokop G. Modeling human vehicle driving by model predictive online optimization. Vehicle System Dynamics. 2001;35(1):19–53.
- [66] Kelly D. Lap time simulation with transient vehicle and tyre dynamics [dissertation]. Cranfield University; 2008.
- [67] Timings J, Cole D. Robust lap-time simulation. Proceedings of the Institution of Mechanical Engineers, Part D: Journal of Automobile Engineering. 2014;228(10):1200–1216.
- [68] Velenis E, Tsiotras P. Minimum time vs maximum exit velocity path optimization during. In: 2005 IEEE international symposium on industrial electronics; June. Dubrovnic, Croatia: IEEE; 2005. p. 355–360.
- [69] Velenis E, Tsiotras P, Lu J. Optimality properties and driver input parameterization for trail-braking cornering. European Journal of Control. 2008;4:308–320.
- [70] Tesi A, Vinattieri F, Capitani R, Annicchiarico C. Development of an e-LSD control strategy considering the evolution of the friction torque with the wear depth. SAE International Journal of Engines. 2016;9(2016-01-1136).
- [71] Global optimization toolbox: User’s guide (r2017a). The MathWorks; 2017. Report no.:
- [72] Patterson MA, Rao AV. GPOPS-II: A matlab software for solving multiple-phase optimal control problems using hp-adaptive gaussian quadrature collocation methods and sparse nonlinear programming. ACM Transactions on Mathematical Software. 2014 October;41(1):1–37.
- [73] Hockenheim. <http://www.hockenheimring.de/en/history/>. 2017; [Online; accessed 31-March-2017]; Available from: <http://www.hockenheimring.de/en/history>.
- [74] Nürburgring. <http://www.nuerburgring.de/en/fans-info/history.html>. 2017; [Online; accessed 31-March-2017]; Available from: <http://www.nuerburgring.de/en/fans-info/history.html>.
- [75] Trabesinger A. Formula 1 racing: Power games. Nature. 2007 June;447(7147):900–903.

## Appendix A. Simulation Parameters

In this appendix, the parameters used in simulation are presented.

Table A1. Vehicle parameters used for simulation.

Parameter	Description	Units	Value
$m$	Mass	$kg$	660
$I_{zz}$	Yaw inertia	$kgm^2$	450
$L$	Wheelbase	$m$	3.4
$a$	Distance of Cg to front axle	$m$	1.8
$b$	Distance of Cg to rear axle	$m$	1.6
$h_{cg}$	Height of the Cg	$m$	0.3
$w_f$	Half front track width	$m$	0.73
$w_r$	Half rear track width	$m$	0.73
$kt_{driving}$	Rear axle torque distribution while driving	-	1
$kt_{braking}$	Rear axle torque distribution while braking	-	0.4
$P_{eng}$	Maximum engine power	$kW$	460
$C_L$	Coefficient of lift	-	3
$C_D$	Coefficient of drag	-	0.9
$A$	Vehicle frontal area	$m^2$	1.5
$\rho$	Air density	$kg/m^3$	1.2
$a_a$	Distance of Cp to front axle	$m$	1.9
$b_a$	Distance of Cp to rear axle	$m$	1.5
$k_d$	Differential coefficient	$Nm/(rad/s)$	10.47
$D$	Proportion of front axle load transfer	-	0.5
$R$	Effective rolling radius of the tire	$m$	0.33

Table A2. Control scheme parameters used in simulation.

Parameter	Description	Units	Value for Hockenheim	Value for Nürburgring
$s_{horizon}$	MPC horizon	$m$	200	250
$s_{MPC}$	MPC update interval $s_{MPC} = (s_f - s_0)/N$	$m$	10	10
$s_0$	Initial distance	$m$	-200	-200
$s_{start}$	Timing start distance	$m$	0	0
$s_{finish}$	Timing stop distance	$m$	2640	4501